symmetry

MDPI

Article

Numerical Study on the Reinforcement Measures of Tunneling on Adjacent Piles

Hongsheng Qiu [1], Zhe Wang [1,*], Mo'men Ayasrah [2,3,*], Chuanbang Fu [4] and Luo Gang [1]

[1] School of Transportation and Logistics Engineering, Wuhan University of Technology, Wuhan 430063, China; 2755@whut.edu.cn (H.Q.); luogang1997@whut.edu.cn (L.G.)
[2] Communication and Transportation Engineering, School of Transportation, Wuhan University of Technology, Wuhan 430063, China
[3] Department of Civil Engineering, Faculty of Engineering, Al al-Bayt University, Mafraq 25113, Jordan
[4] China Municipal Engineering Zhongnan Design & Research Institute Co., Ltd., Haikou 570105, China; 249146@whut.edu.cn
* Correspondence: zhewang1001@whut.edu.cn (Z.W.); ayasrahmomen@whut.edu.cn (M.A.)

Abstract: Tunnel construction will inevitably change the surrounding soil's original stress and displacement fields, affecting the surrounding piles. In addition, the lateral displacement of the soil at the subway tunnel's face is symmetrically distributed along the tunnel's central axis, which is greater in the center and smaller on both sides. Therefore, the protection of existing piles and providing a reasonable reinforcement plan have become the focus of attention. Taking a section of Tianjin Metro Line 3 as the research object, this paper studies the influence of the shield tunnel excavation process on the existing pile foundation through three-dimensional finite element simulation. The model has been verified through field monitoring data. Then, parameter analysis has been carried out for two reinforcement measures: grout reinforcement and isolation pile construction. According to the research results, the impact of shield construction on the pile foundation is mainly within the range of twice tunnel diameter to the pile foundation from the front and back of the tunnel face. In addition, the grouting reinforcement has better control of the vertical displacement of the existing pile foundation. The construction of isolation piles can better control the lateral displacement of the existing pile foundation. Have certain reference significance for similar projects.

Keywords: tunnel construction; numerical simulations; adjacent piles; grouting reinforcement; isolation pile

Citation: Qiu, H.; Wang, Z.; Ayasrah, M.; Fu, C.; Gang, L. Numerical Study on the Reinforcement Measures of Tunneling on Adjacent Piles. *Symmetry* **2022**, *14*, 288. https://doi.org/10.3390/sym14020288

Academic Editor: Jan Awrejcewicz

Received: 29 December 2021
Accepted: 25 January 2022
Published: 31 January 2022

1. Introduction

Due to rising urban population density and severe traffic congestion, Chinese tunnels have seen remarkable growth in recent years [1,2], with more tunnels being built as subsurface developments [3–8]. However, the surrounding environment is complicated. Therefore, the tunneling construction unavoidably ruins the surrounding soil's original stress and displacement fields [3], which is the main part that bears the unloading stress. The lateral displacement of the soil at the subway tunnel's face is symmetrically distributed along the tunnel's central axis, which is greater in the center and smaller on both sides. Hence, improving the self-supporting capability of surrounding soil and controlling deformation can effectively lessen the impact of tunnel construction on the surrounding environment and, at the same time, extend the service life of the tunnel during operation [5]. Therefore, tunnel-related soil deformation control in the process of tunnel excavation and support has emerged as a challenge that requires special attention [9]. Since tunnel excavation and support may significantly influence the surrounding piles, reinforcing the surrounding piles is also a significant problem [10,11]. Many researchers have carried out numerical research analysis methods for this problem [12–20], as well as some centrifuge model

tests [21–24], and field observations [25,26] have been used to investigate the impact of the nearby pile foundations under shield tunneling.

It is worth mentioning that, if the distance between the existing pile foundation and the shield tunnel is too close, the pile foundation may have an uneven settlement, structural deformation, and even cracks with the tunnel excavation [27–29]. In order to ensure the smooth excavation of the tunnel and protect the safety of adjacent pile foundations, some reinforcement measures must be taken [30–38]. Therefore, the protection of existing piles and providing a reasonable reinforcement plan have become the focus of attention.

In this paper, a 3D finite element model is provided to analyze the displacement reinforcement effect through two different reinforcement measures on the pile foundations. The parameters of the 3D model are based on the Modified Mohr–Coulomb constitutive model, which can better simulate the unloading of soil mass and redistribution of stress during the tunnel excavation. Before the parameter study, the 3D model was verified by field test data, and the deformation degree of the existing pile foundation was analyzed as the shield tunnel was excavated. The grouting reinforcement and isolation pile reinforcement of existing pile foundations have been studied parametrically. In addition, the effects of the two reinforcement measures on the displacement of the pile foundation under different parameters were analyzed and compared.

2. Overview of the Engineering

The Tianjin Metro-Line 3 and Adjacent Abutment

Tianjin Metro Line 3 is the city's main metro line, alleviating traffic congestion and making transit more convenient for inhabitants. With a length of 33.7 km, the Tianjin Metro Line 3 was constructed using a shield Tunnel Boring Machine (TBM), as shown in Figure 1. The tunnel's external and internal diameters are 6.20 and 5.60 m, respectively. The prefabricated section liner has a thickness of 0.35 m. In this study, a segment of Tianjin Metro Line 3 passes near the viaduct. The distance between the viaduct abutment and the tunnel is 1.23 m, while the distance between the pile foundation and the tunnel is 1.58 m. The abutment is supported by eight 0.35 m × 0.35 m square piles; the abutment's dimensions are 4.2 m in length, 2.8 m in width, and 1.35 m in height. The abutment's design allowable load capacity is 340 kN. Figure 2 shows the positional relationship between the tunnel and the pile foundation.

Figure 1. The location of Tianjin Metro Line 3.

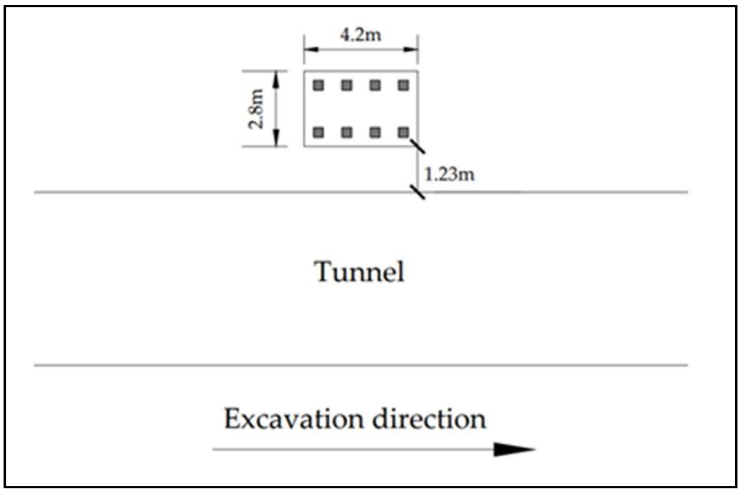

Figure 2. The position relative to the tunnel route.

The length of each pile is 25 m, the nearest distance between the pile and the tunnel is 1.58 m, the depth of the tunnel is 8 m, and the thickness of the precast segmental lining is 0.3 m.

Figure 3 shows the positional relationship between the sections of the tunnel and the pile foundation and presents the conditions of the soil layers. The soil layer properties are adopted from the study by [39], which used field SPT and laboratory tests. The soil layers are dominated by miscellaneous fill and silty clay, etc. The overall nature of the soil is relatively weak.

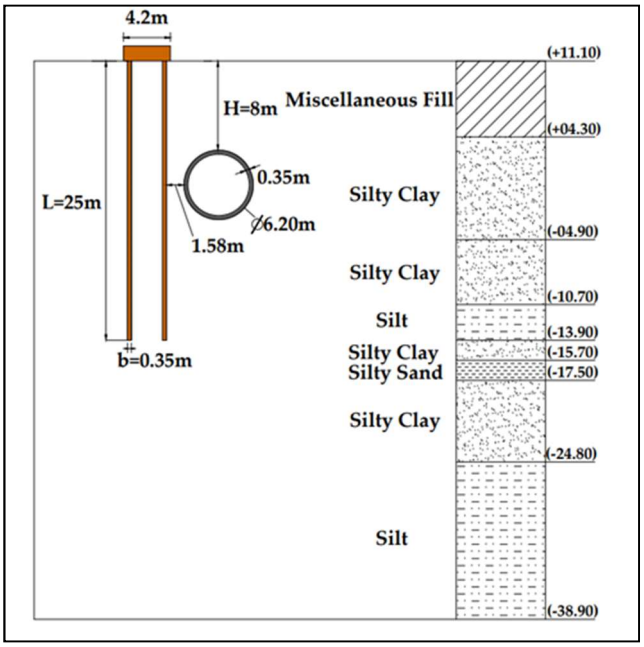

Figure 3. Engineering geological profile (unit: m).

3. Finite Element Modeling

3.1. Numerical Model

According to the Tianjin Metro Line 3 project overview, a certain section of the tunnel passes through the pile foundation of the viaduct abutment. A three-dimensional model is established to study the effects of tunnel construction on pile foundations using the Midas GTS-NX finite element package. Considering the boundary effect on the accuracy of the numerical results, the influence of tunnel construction on adjacent pile foundations is

chosen to establish a 3D finite element model. In this study, the numerical model is shown in Figure 4. The mesh used in this model consists of 52,045 nodes and 49,075 elements. The mesh dimensions are 60 m (≈9.75 D) wide in the transverse direction, 72 m (≈11.75 D) in the longitudinal direction, and 42 m (≈6.75 D) deep in the vertical direction. Therefore, these dimensions are sufficiently large to minimize boundary effects in the numerical modeling because the massive raise in mesh size does not cause any change in the analysis results. In numerical modeling, the soil layer, tunnel lining, and cap are simulated as continuum solids while the piles foundation are simulated with beam elements, and the shield machine is considered as a continuum shell. The pile interface is set between the pile and the soil.

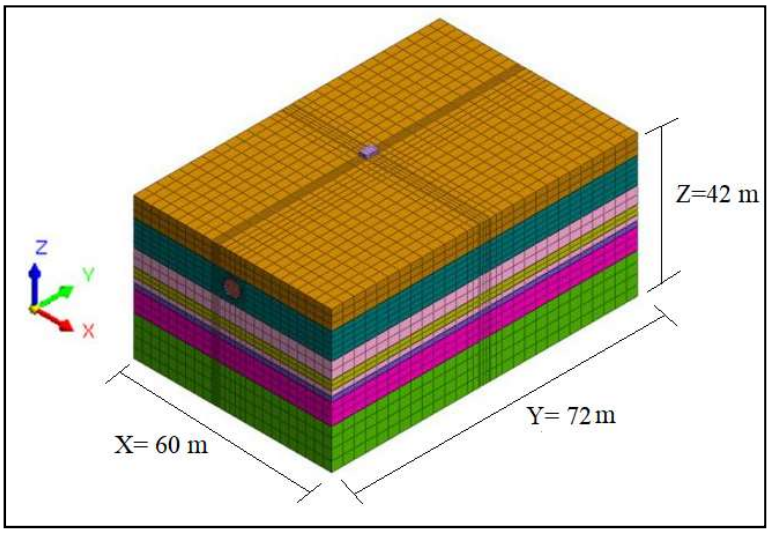

Figure 4. 3D finite element model.

The boundary conditions are set as follows: the top side is a free surface, the four side surfaces restrain its normal displacement, and the bottom surface restrains the displacement in three directions. Only the self-weight stress is considered in the initial stress field. Because the existence of groundwater only affects the bulk density of the soil, the seepage effect of groundwater is not considered.

The average buried depth of the tunnel is 8 m, the diameter of the tunnel is 6.2 m, the thickness of the segment is 0.3 m, and the distance between the axis of the tunnel and the ground is 11.1 m. The whole shield excavation process is divided into 27 steps in total. The excavation footage outside the scope of the pile cap is set to 4 m. For more accurate research and analysis of the impact of shield excavation on the pile foundation, the excavation footage within the scope of the pile cap is set to 2 m. During the shield tunneling process, the pressure of the shield machine on the tunnel face to simulate the pressure of the earth is set to 100 Kpa uniform stress. The shield machine digs a step every time it assembles the sections and grouts at the tail of the shield. The grouting pressure generated by the soil is simulated with uniform compressive stress of 200 Kpa. Considering the segments need to be assembled in the actual construction, it will have a certain impact on the overall stiffness of the lining, so the elastic modulus of the segment is taken as a reduction factor of 0.85 [40], and the elastic material is used to simulate the elastic modulus of the segment E = 25.9 Mpa, with the Poisson's ratio of the segment being 0.2. The activation and passivation function of the software is carried out to simulate tunnel excavation, activate the corresponding shield shell, segment, and corresponding face pressure, segment pressure, and grouting pressure during each excavation step. At the same time, part of the soil is passivated during excavation and the segment and shield shell grid group is transformed to the proper segment and grouting layer properties by changing the grid properties during segment grouting and assembling.

3.2. Constitutive Models and Material Parameters

The accuracy of the numerical calculation is affected by selecting the constitutive model. The tunnel is a dynamic excavation and unloading process in the shield construction. The soil parameters of this 3D model adopt the Modified Mohr–Coulomb constitutive. The Modified Mohr–Coulomb constitutive can take into account the shear hardening compared with the Mohr–Coulomb constitutive. The effects of the shear and density hardening mechanisms can better simulate the properties of various types of soil, including soft soil and hard soil, to better reflect the unloading rebound phenomenon during tunnel shield excavation [20]. The Modified Mohr–Coulomb constitutive model considers three different soil stiffness parameters: triaxial loading stiffness, oedometer loading modulus, and unloading-reloading modulus. Under normal circumstances, E_{oed} and E_{50} take the same value, and E_{ur} takes three times the value of E_{50} [41]. Using the undrained Young's modulus, E_u of the soil can be calculated according to Equation (1):

$$E_u = k\, C_u \tag{1}$$

where C_u is undrained shear strength, kN/m^2, and k is a factor from Duncan chart, unitless [42].

The Modified Mohr–Coulomb constitutive parameters of the weighted average soil layer are shown in Table 1. The coefficient of lateral earth pressure (k_o) at rest is determined by Mayne and Kulhawy (1982) [43]. The natural gravity, cohesion c, friction angle φ, and Poisson's ratio ν of the soil are calculated by mathematical equations. According to site survey data, the physical characteristics of the soil strata are summarized in Table 1.

Table 1. Soil layers engineering parameters.

Soil Layers	Thick (m)	Density /(kN/m^3)	Cohesion Force (kPa)	Poisson's Ratio	Frictional Angle (°)	E_{oed} (MPa)	E_{50} (MPa)	E_{ur} (MPa)	Lateral Earth Pressure Coefficient
Miscellaneous Fill ①	6.8	19.20	14	0.31	15.2	2.31	2.31	6.93	0.532
Silty clay ①	9.2	19.10	28	0.30	34.5	3.45	3.45	10.35	0.420
Silty clay ②	5.8	20.20	6	0.34	11.8	14.59	14.59	43.77	0.385
Silt ①	3.2	20.50	11	0.35	12.7	13.67	13.67	41.01	0.385
Silty clay ③	1.8	20.30	30	0.28	11.9	6.20	6.20	18.6	0.412
Silty sand ①	1.8	21.50	6	0.32	21.2	12.02	12.02	36.06	0.420
Silty clay ④	7.3	20.50	8	0.3	13.2	5.69	5.69	17.07	0.385
Silt ①	14.1	20.30	7	0.29	27.2	14.60	14.60	43.8	0.420

The pile foundation adopts general beam elements, the segments adopt solid elements, and the shield shell and grouting elements adopt two-dimensional plate elements. The piles and the cap use C30 concrete, and the tunnel segments use C50 concrete. The specific material parameters are shown in Table 2.

Table 2. The specific material parameters.

Material	Elastic Modulus/(MPa)	Unit Weight/(kN/m^3)	Poisson's Ratio
C30 concrete	3×10^5	23.5	0.20
Grouting	2.1×10^2	23	0.25
Shield shell	2.6×10^5	78	0.30
Lining	2.89×10^4	24.5	0.20

4. Verification of the Numerical Model

To ensure the authenticity of the calculation results and verify the validity of the 3D model, it is necessary to compare the on-site monitoring data with the settlement values of the monitoring points in the simulation calculation results. In order to monitor the displacement of the bridge abutment and construction safety during the tunnel construction, four monitoring points were arranged above the bridge cap to observe the horizontal and vertical displacements as shown in Figure 5.

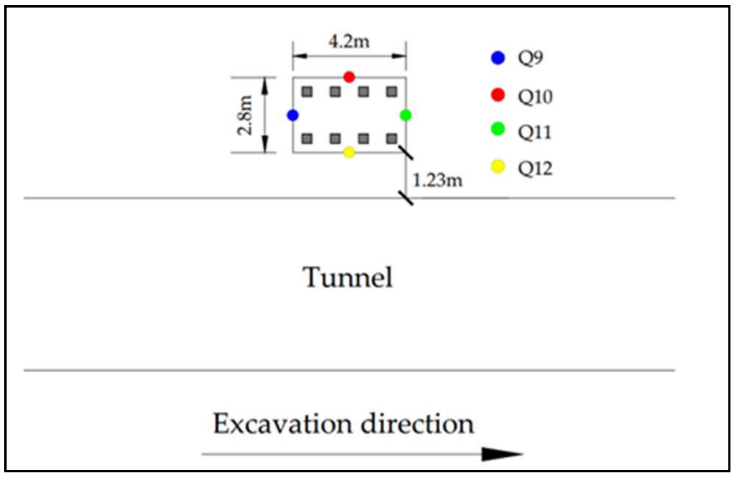

Figure 5. The layout of the pile cap monitoring point.

The comparison between the measured settlement data and the vertical displacement in the numerical simulation of Q9 and Q12 points is shown in Figures 6 and 7, respectively. It can be seen from the two figures that the impact of shield construction on the pile foundation is mainly within the range of twice the tunnel diameter from the front and back of the tunnel face to the pile foundation. Additionally, the settlement at this stage accounts for about three-quarters of the total settlement. Numerical calculation results are slightly different from actual measured data, which verifies the validity of the model parameters selection and working condition settings, and the authenticity of the calculation results.

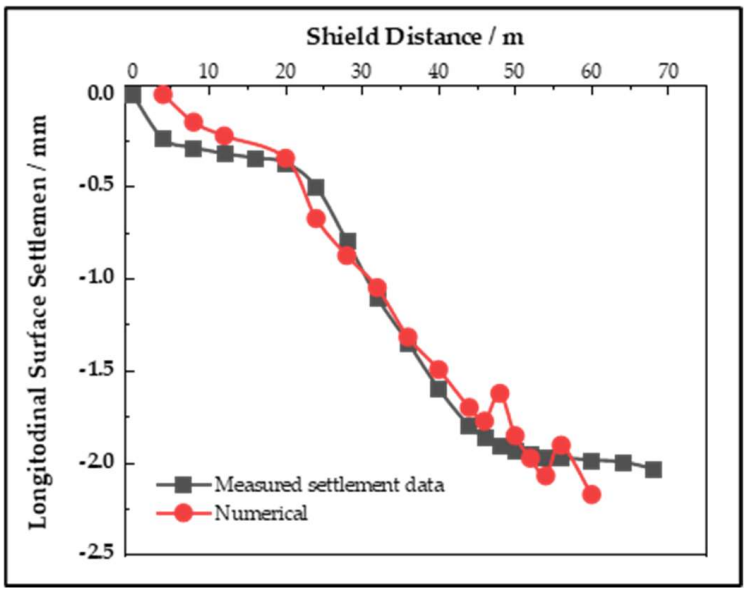

Figure 6. The longitudinal surface settlement at different points relative to tunnel advancement of Q9 point.

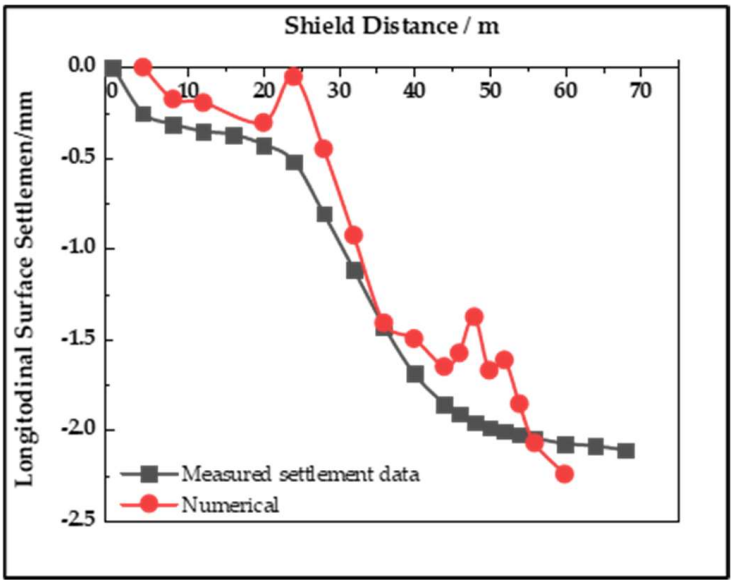

Figure 7. The longitudinal surface settlement at different points relative to tunnel advancement of Q12 point.

5. Numerical Results and Discussion

To simplify the calculation and improve the analysis efficiency, adjust the distance to 6 m between the tunnel and the pile. The soil layers are combined into one layer in the new 3D model, taking the weighted average of soil parameters according to the thickness of each layer. The other parameters are simulated according to the actual situation, analyzing the influence of tunnel construction on the deformation of the pile foundation.

Taking the coordinate axis X as the lateral direction, the lateral displacement of the pile foundation is positive along the axis X, which means the direction towards the tunnel is positive, and the opposite direction of axis X is negative; along the tunnel, the axis is taken as the longitudinal direction, and the shield direction is the positive direction; along the coordinate axis, Z is taken as the vertical direction. The settlement displacement of the pile is taken as negative.

5.1. The Influence of Tunnel Construction on Deformation of the Pile Foundation

When the tunnel is excavated forward, the lateral displacement trend of the pile foundation is shown in Figure 8. Among the figure, D is the excavation face passing through the pile position one time the tunnel diameter and −D is the excavation face not passing through the pile position one time the tunnel diameter.

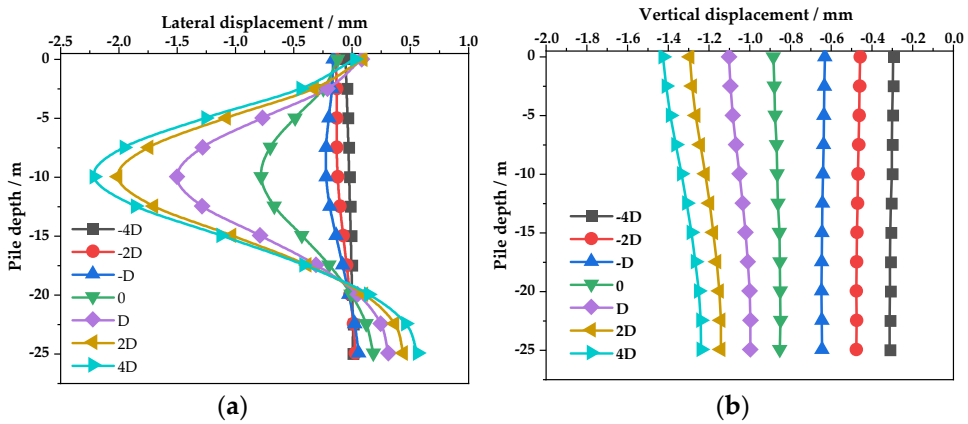

Figure 8. The displacement of the pile at different construction stages: (**a**) lateral displacement; (**b**) vertical displacement.

It can be seen from Figure 8a that when the excavation face is −2D from the position of the pile foundation, the excavation has little influence on the lateral displacement of the pile foundation, and the influence gradually increases thereafter. The most affected area is mainly concentrated between −D and 2D and reaches the maximum value at the tunnel axis. After tunnel excavation, the pile body is inclined to the side of the tunnel as a whole, the reason being that the tunnel excavation due to the soil at the top of the tunnel is settling and the soil at the bottom of the tunnel is uplifted. The large lateral displacement of the pile foundation away from the tunnel is due to the pushing effect of the soil, and the lateral displacement of the upper part of the pile towards the tunnel is driven by the settlement of the soil at the top of the tunnel.

On the other hand, as shown in Figure 8b when the excavation surface reaches the position of the pile foundation, the increase in the settlement value of the pile foundation is basically the same. This means the settlement of the pile is an overall settlement. When the excavation surface reaches the pile surface, the settlement value of the pile top gradually grows larger than the settlement value of the pile bottom and the maximum settlement difference is 0.213 mm, indicating the pile is compressed. The reason for this is the uplift of the soil under the tunnel.

5.2. The Effect of Grouting Reinforcement on Deformation of the Pile Foundation

Grouting reinforcement is commonly used in support of pile foundations. It refers to injecting the configured concrete grout into the soil around the pile foundation through a grouting pipe and then changing the soil from loose to dense—which means increasing the strength of the soil around the pile. The diameter of the grouting holes on both sides of the pile foundation is 0.08 m, the grouting pressure is 0.3 MPa, the water–cement ratio is 0.7, and the diffusion radius is 1 m.

5.2.1. The Effect of Grouting Reinforcement Depth on Deformation of the Pile Foundation

In this study, the grouting reinforcement is simulated by changing the soil properties within 2 m of the pile circumference. The elastic modulus of the soil after grouting is taken as 300 MPa. The depth of grouting reinforcement is respectively taken as 0.75 H, 1 H, 1.25 H, and 1.5 H, where H is the average buried depth of the tunnel center-line, so H is 11.1 m. The soil reinforcement analysis model around the pile (soil mesh groups are hidden) is shown in Figure 9.

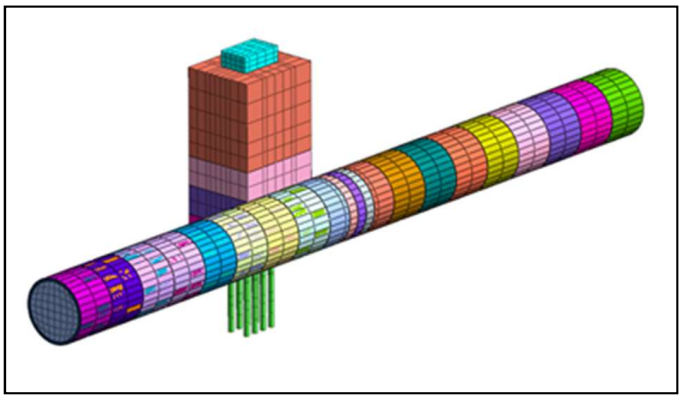

Figure 9. Finite element model of grouting reinforcement.

Because the deformation of the front row piles during shield tunneling is greater than that of the rear row piles, we take the front row piles as the research object in this study. Under different conditions of grouting reinforcement depth, the lateral displacement and vertical displacement of the front row of piles are shown in Figure 10. It can be seen from Figure 10a that as the depth of grouting reinforcement continues to increase, the lateral displacement of the front piles gradually decreases, but when the reinforcement

depth exceeds 1.25 H, the reinforcement effect will be weakened to a certain extent as the reinforcement depth increases. It can be seen from Figure 10b that when grouting is not used for reinforcement, the maximum vertical displacement of the pile top is 1.40 mm, and the settlement value of the pile bottom is 1.22 mm. During grouting reinforcement, as the reinforcement depth increases, the vertical displacement of the pile top gradually decreases. When the reinforcement depth exceeds 1 H, the settlement at the bottom of the pile is slightly larger than the settlement at the top of the pile. At this time, the force of the pile foundation changes from compression-oriented to tension-oriented.

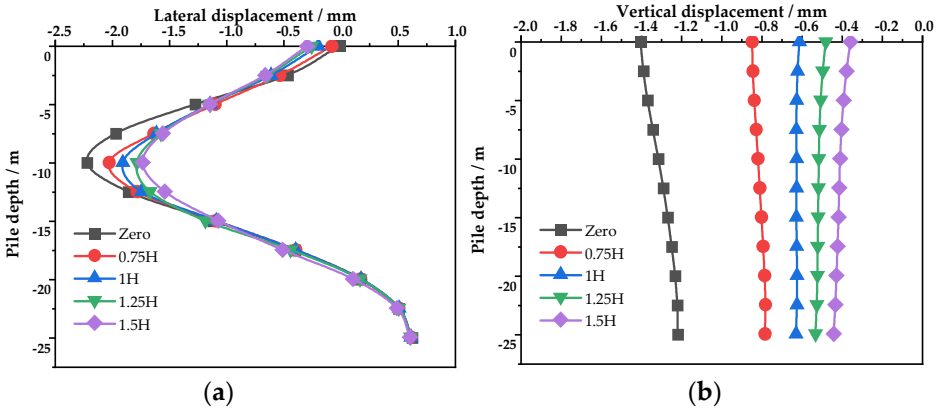

Figure 10. The displacement of piles under different grouting depths: (**a**) lateral displacement; (**b**) vertical displacement.

In order to better understand the reinforcement effect under different reinforcement depth conditions, we introduce the reinforcement effect parameter as reinforcement rate ω to describe the reinforcement effect of the pile foundation. The calculation Equation (2) is as follows:

$$\omega = \frac{|x_i - x_0|}{x_0} = \frac{\Delta x}{x_0}, \tag{2}$$

where x_0 represents the maximum lateral displacement of the pile before reinforcement, x_i represents the maximum displacement of the pile after reinforcement, and Δx represents the maximum displacement value of the pile after soil reinforcement and when it is not reinforced.

Under different grouting reinforcement depths, the reinforcement rate of the lateral displacement of the front row of piles and the reinforcement rate of the vertical displacement of the pile top are shown in Figure 11. When the reinforcement depth is 1.25 H, the pile lateral displacement reinforcement rate increases most obviously, with the reinforcement rate being 19.8%. When the reinforcement depth is increased to 1.5 H, the pile shaft lateral displacement reinforcement rate is only 2.3% higher than that of 1.25 H, and the effect is not significant. When the reinforcement depth is above 1 H, every time the reinforcement depth increases by 0.25 H, the pile top reinforcement rate will increase by about 9.3%. The reinforcement effect is the best at 1.5 H, reaching 75.0%. Considering the vertical and horizontal displacement of the pile foundation comprehensively, we recommend that the grouting reinforcement depth be 1.25 H.

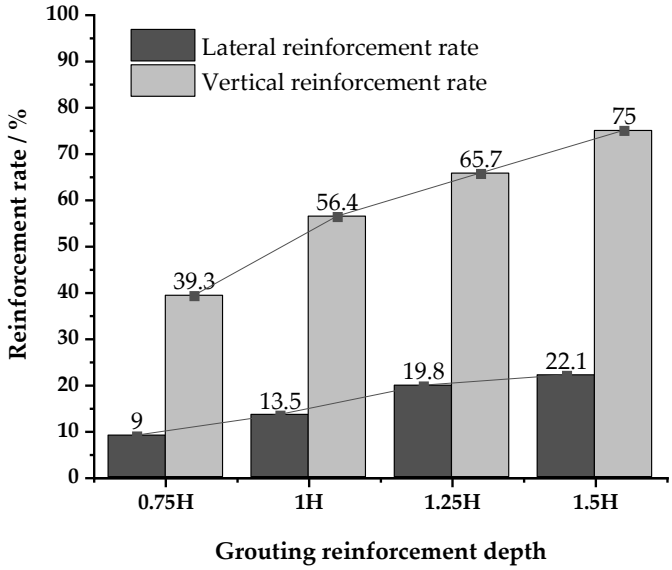

Figure 11. The displacement reinforcement rate of the pile under different grouting depths.

5.2.2. The Effect of Grouting Reinforcement Area on Deformation of the Pile Foundation

The scope of grouting reinforcement refers to grout in the different areas around the abutment, which is divided into four different grouting reinforcement areas in this study. Determining different grouting areas by a different arrangement of grouting holes, the design of plans is shown in Figure 12. The grouting reinforcement depth is 1.25 H.

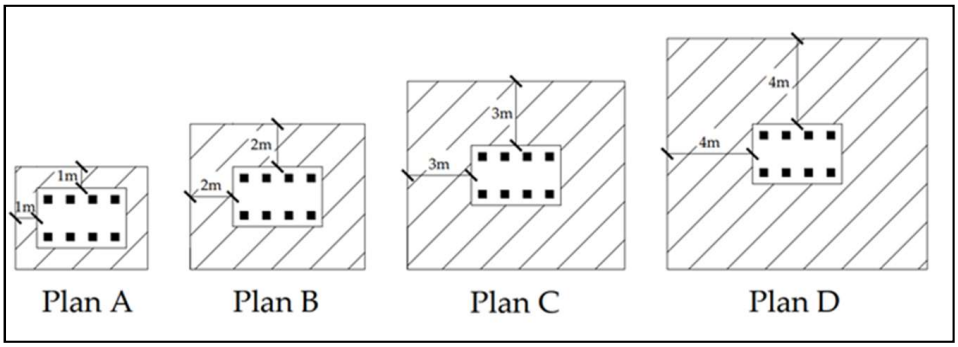

Figure 12. Four plans of different grouting reinforcement areas.

Figure 13 presents the changes in the lateral displacement and vertical displacement of the pile foundation as the area of grouting reinforcement changes. The maximum lateral displacement of the pile foundation decreases with the increase of the grouting reinforcement range, and the maximum displacement is located at the pile's −10 m, but the lateral displacement of the pile top decreases with the increase of the reinforcement area, indicating that when the grouted area increases, the integrity of the pile foundation and the surrounding soil is stronger, and the stress is more dispersed. The vertical displacement of the pile decreases with the increase of the reinforcement area, but the displacement of the top of the pile gradually grows smaller than the displacement of the bottom of the pile, indicating that the pile foundation changes from compression to tension with the increase of the grouting reinforcement area.

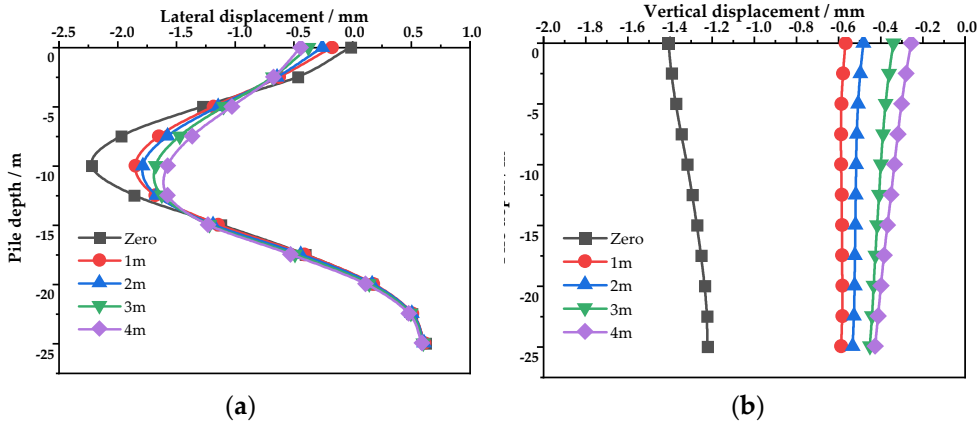

Figure 13. Lateral displacement of piles under different grouting areas: (**a**) lateral displacement; (**b**) vertical displacement.

The histogram of the pile's lateral reinforcement rate and vertical reinforcement rate in the case of different grouting reinforcement areas is shown in Figure 14. The lateral reinforcement rate of piles increases with the increase of the grouting area and reaches the maximum when the reinforcement area is 4 m. The maximum lateral reinforcement rate is 82.1% and the maximum vertical reinforcement rate is 29.2% for each increase in the grouting area. The lateral reinforcement rate increases by 4.17%, and the vertical reinforcement rate increases by 7.4%.

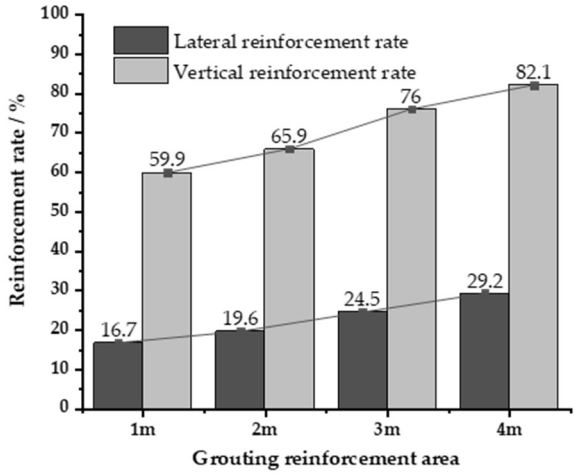

Figure 14. The displacement reinforcement rate of the pile under different grouting areas.

5.3. The Effect of Isolation Pile on Deformation of the Pile Foundation

The construction of isolation piles can assist the reinforced pile foundation to bear the lateral pressure of the soil, reducing the soil displacement around the pile foundation caused by shield construction. The construction is economical and effective and is widely used in various reinforcement projects. The isolation piles are used in static pressure piles, and implanted beam elements are used in the numerical calculation—the boundary conditions restrict its rotation in the Z direction. During isolation pile reinforcement, the main influencing factors are the pile diameter D of the isolation pile, the elastic modulus E, the pile length L, the isolation pile spacing X, and the minimum horizontal distance S between the isolation pile and the tunnel. In this study, the pile diameter D and elastic modulus E of the isolated pile are not changed. The control variable method is used to study the influence of other influencing parameters on the reinforcement effect. The pile diameter of the isolated pile is D = 1 m, and the elastic modulus is E = 30 GPa. The 3D model of isolation pile reinforcement (soil mesh groups are hidden) is shown in Figure 15.

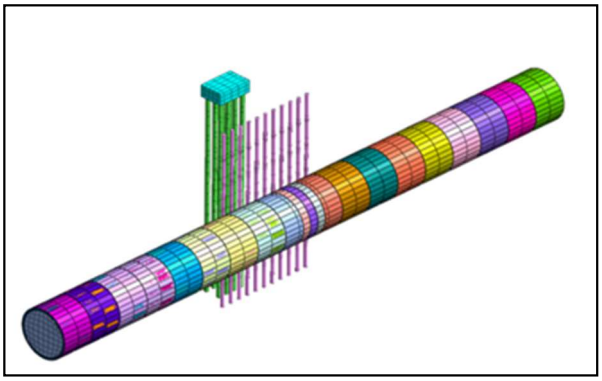

Figure 15. The 3D model of isolation pile reinforcement.

5.3.1. The Influence of Isolation Pile Length on Pile Foundation Reinforcement

To study the effect of isolation pile length on pile foundation reinforcement, the minimum horizontal distance between the isolated pile and the tunnel is 1 m, and the distance between the isolated piles is 1.2 m. The lengths of the isolation piles are respectively 1 H, 1.25 H, 1.5 H, and 1.75 H. Figure 16a shows the lateral displacement of the pile under different isolation pile lengths. The maximum lateral displacement of the pile decreases with the increase of the length of the isolation pile and reaches the minimum at 1.75 H, which is 1.68 mm. The lateral displacement of the pile top and the bottom of the pile increases to a certain extent with the increase of the length of the isolation pile, which indicates that the length of the isolation pile has a certain spreading effect on the stress of the pile foundation.

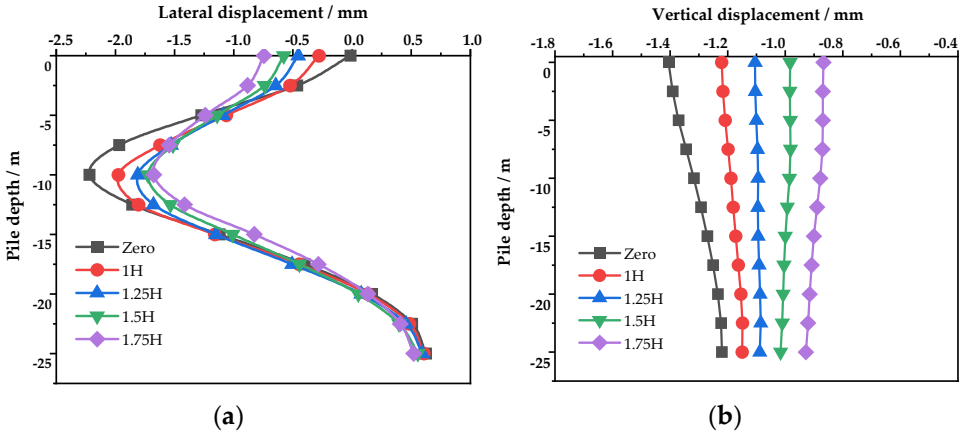

Figure 16. The displacement of the pile under different isolation pile lengths: (**a**) lateral displacement; (**b**) vertical displacement.

Figure 16b shows the vertical displacement of the pile under different isolation pile lengths. The maximum vertical displacement of the pile decreases with the increase of the length of the isolation pile and reaches the minimum at 1.75 H, which is 0.93 mm. As the length of the isolation pile increases, the vertical displacement of the top of the pile grows gradually greater than the vertical displacement of the bottom of the pile, indicating that the pile foundation has changed from a compression state to a tension state.

Figure 17 shows the trend of the maximum lateral displacement reinforcement rate of the pile and the reinforcement rate of the top of the pile as the length of the isolation pile changes. For every 0.25 H increase in the length of isolation piles, the horizontal reinforcement rate increases by an average of 8.4%, and the vertical reinforcement rate increases by an average of 12.3%. The length of the isolation pile reaches its maximum value at 1.75 H, the lateral reinforcement rate is 57.9%, and the vertical reinforcement rate is 36.2%.

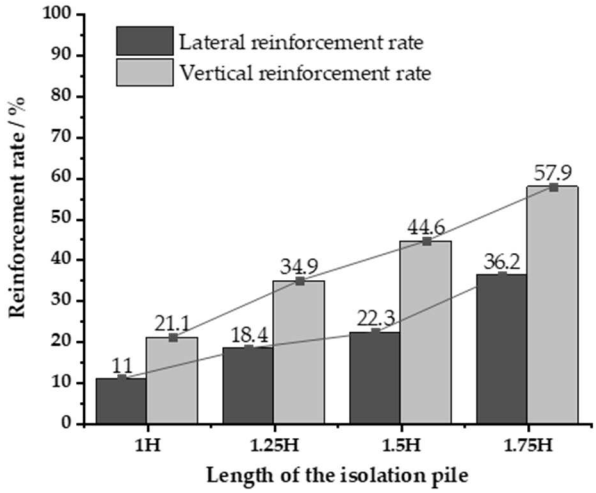

Figure 17. The displacement reinforcement rate of the pile under different lengths of the isolation pile.

5.3.2. The Influence of Isolation Pile Spacing on Pile Foundation Reinforcement

To understand the effect of isolation pile spacing X on pile foundation reinforcement, the minimum horizontal distance is 1 m between the isolation pile and the tunnel. The isolation pile length is taken as L = 1.75 H in the above analysis.

Figure 18a shows the lateral displacement of the pile under different isolation pile spacing conditions. When S is below 4D, the maximum lateral displacement does not change significantly with the increase of S. When S exceeds 5D, the maximum lateral displacement becomes larger. This is because when the spacing between the isolation piles is too large, their row effect is weakened, and the soil on both sides of the pile cannot be effectively prevented from side-slip displacement, resulting in the reinforcement effect being weakened.

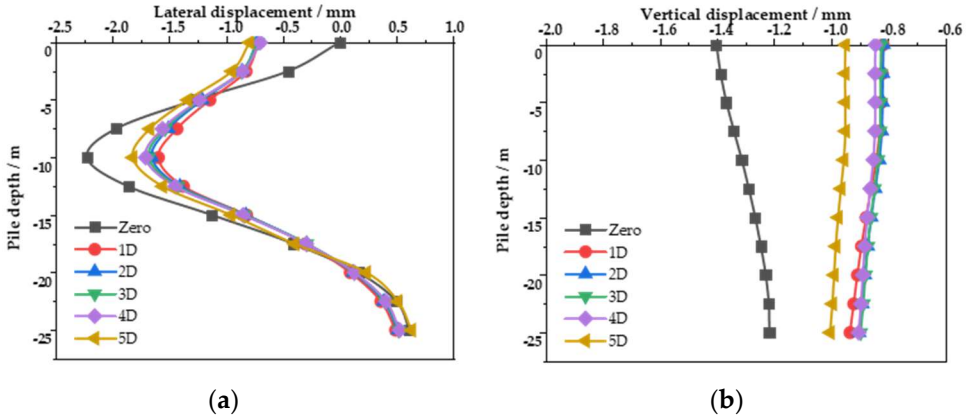

(**a**) (**b**)

Figure 18. The displacement of the pile under different spacing of the isolation pile: (**a**) lateral displacement; (**b**) vertical displacement.

Figure 18b shows the vertical displacement curve of the pile under different spacing of the isolation pile. Under the action of the isolation pile, the pile foundation changes from compression to tension in the vertical direction. When S is below 4D, the vertical displacement of the pile does not change significantly with the increase of S. When S exceeds 5D, the vertical displacement increases. This is because when the spacing between the isolation piles is too large, the pile row effect is weakened, the soil on both sides of the isolation pile cannot be effectively prevented from side-slip displacement, and the reinforcement effect is weakened.

Figure 19 shows the displacement reinforcement rate of the pile under different spacing of the isolation pile. The pile reinforcement rate does not change significantly when the

spacing between isolated piles is less than 4D. The lateral displacement reinforcement rate averages 25.3%, and the vertical displacement reinforcement rate averages 40.1%. When the spacing between isolated piles becomes 5D, the pile reinforcement rate suddenly decreases, the lateral reinforcement rate becomes 18.1%, and the vertical reinforcement rate becomes 32.2%.

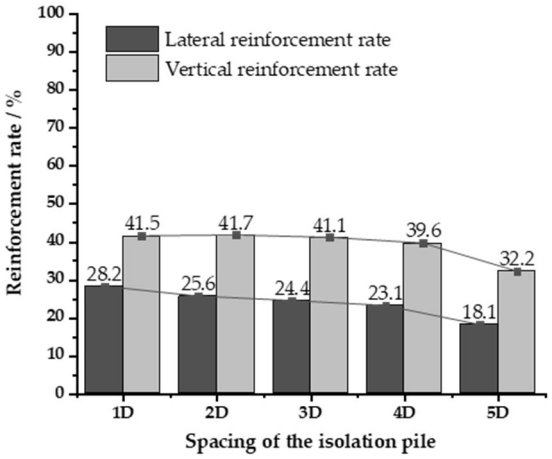

Figure 19. The displacement reinforcement rate of the pile under different spacing of the isolation pile.

5.3.3. The Influence of Horizontal Distance between the Isolation Pile and the Tunnel (S) on Pile Foundation Reinforcement

To study the influence of the horizontal distance between the isolation pile and the tunnel on the pile foundation reinforcement effect, the isolation pile length design is set as L = 1.75 H, the isolation pile spacing design as X = 1.2 m, and the pile diameter design as =0.4 m. As shown in Figure 20a, the lateral displacement of the pile foundation gradually becomes larger as S increases. The maximum lateral displacement of the pile is 1.69 mm when S is 1 m, and the maximum lateral displacement of the pile becomes 2.09 mm when S is 5 m.

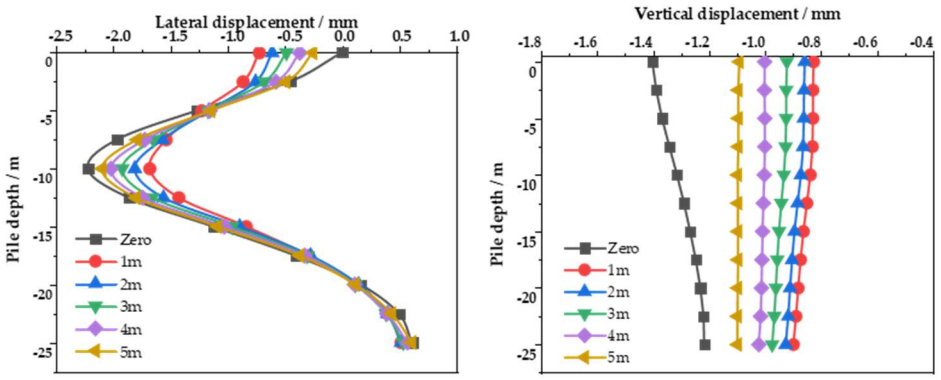

(**a**) (**b**)

Figure 20. The displacement of the pile under different distances between the isolation pile and the tunnel: (**a**) lateral displacement; (**b**) vertical displacement.

As shown in Figure 20b, the vertical displacement of the pile gradually increases as S increases, with the maximum vertical displacement being 1.09 mm and the overall settlement of the pile being uniform when S is 5 m. Therefore, the farther the isolation pile is from the tunnel, the weaker the reinforcement effect on the pile foundation and, as the isolation pile is farther from the tunnel, the uneven vertical settlement of the pile foundation gradually weakens.

As shown in Figure 21, the pile reinforcement rate decreases as S increases, and the lateral reinforcement rate changes from 41.1% to 22.1%. The vertical reinforcement rate

of the pile foundation has changed from 24.4% to 5.6%. Therefore, when the isolation pile is used for reinforcement, the closer the isolation pile is to the tunnel, the better the reinforcement effect.

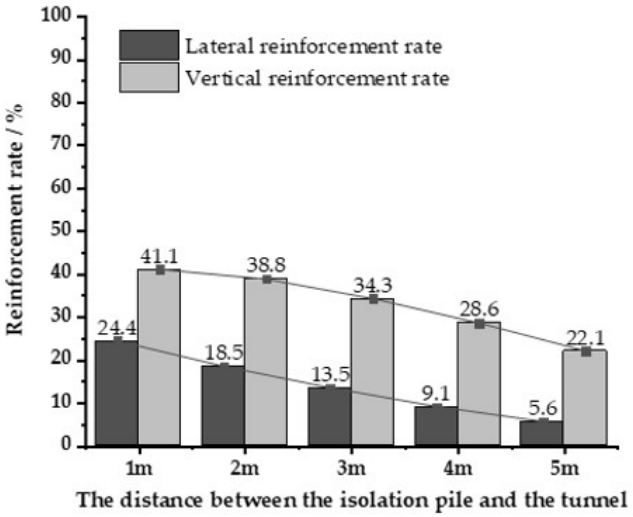

Figure 21. The displacement reinforcement rate of the pile under different distances between the isolation pile and the tunnel.

6. Conclusions

Based on the Tianjin Metro Line 3, this paper studies the reinforcement measures of tunnels passing through adjacent piles. A series of 3D models based on different reinforcement conditions have been conducted by Midas GTS/NX. The conclusion is that the pile is more affected under the shield construction that is first touched by the tunnel face. The impact of shield construction on the pile foundation is mainly within the range of twice tunnel diameter to the pile foundation from the front and back of the tunnel face; the settlement at this stage accounts for about three-quarters of the total settlement. In addition, when the pile foundation is reinforced by grouting, the depth change of the grouting reinforcement is not as effective as the grouting reinforcement area on the pile foundation displacement. The effect of grouting reinforcement on the lateral displacement of the pile foundation is stronger than that of the vertical displacement reinforcement. Furthermore, when isolation piles are used for reinforcement, the length of the isolation piles and the distance from the tunnel have a greater impact on the reinforcement effect of the pile foundation than the isolation piles spacing. However, the spacing of the isolation piles should not be too large; otherwise, the isolation piles will lose the pile row effect, resulting in a significant reduction in the reinforcement effect. Finally, comparing the control effects of isolated piles and grouting reinforcement, isolated piles have better control of the lateral displacement of the pile foundation, and grouting reinforcement has better control of the vertical displacement of the pile foundation.

Author Contributions: Conceptualization, H.Q., Z.W., M.A., C.F. and L.G.; formal analysis, M.A., Z.W. and C.F.; investigation, H.Q., Z.W. and M.A.; writing—original draft preparation, H.Q., M.A. and Z.W.; supervision, H.Q. and L.G. All authors have read and agreed to the published version of the manuscript.

Funding: The publishing of this paper is financially supported by the National Natural Science Foundation of China (No. 11672215).

Institutional Review Board Statement: Not applicable.

Informed Consent Statement: Not applicable.

Data Availability Statement: The data presented in this study are available on request from the corresponding author.

Conflicts of Interest: The authors declare no conflict of interest.

References

1. Liu, B.; Fan, X.; Wang, Y.; Zhang, J.; Fan, Z. Influences of excavation on adjacent existing metro tunnels: A review. *Chin. J. Geo. Eng.* **2021**, *43*, 253–258.
2. Hong, K. State-of-art and Prospect of Tunnels and Underground Works in China. *Tunn. Constr.* **2015**, *35*, 95–107.
3. Huo, J.; Wang, L.; Zhou, S. Safety Analysis of Foundation Reinforcement Scheme for Shield Tunnel Under-Passing Intercity Railway. *Chin. Railw. Sci.* **2011**, *32*, 71–77.
4. Li, D.; He, X.; Qin, L.; Kang, Y.; Zhou, D.; Guo, C. Stability Control of Ultra Shallow-Buried Metro Tunnel with Super Large-Span in Process of Crossing Bridge. *Chin. J. Mech. Eng.* **2013**, *32*, 3636–3642.
5. Song, Q. Study on control measures of the influence of shallow buried tunnel excavation on the subgrade settlement of high-speed railway in operation. *Vibroeng. Procedia* **2021**, *36*, 37–42. [CrossRef]
6. Zhe, W.; Si, F. Finite Element Analysis of Excavation of Shallow Tunnels under the Existing Road. *Adv. Mater. Res.* **2012**, *1615*, 446–449.
7. Zhang, P.; Pan, Y.; Yu, Z.; Guan, X.; Wang, G.; An, J.; Lei, H. Ground subsidence characteristics caused by construction of shallow-buried tunnel in a sandy soil composite formation. *Arab. J. Geosci.* **2020**, *13*, 693–712. [CrossRef]
8. Ayasrah, M.; Qiu, H.; Zhang, X.; Daddow, M. Prediction of Ground Settlement Induced by Slurry Shield Tunnelling in Granular Soils. *Civ. Eng. J.* **2020**, *6*, 2273–2289. [CrossRef]
9. Xu, G.; Li, C.; Wang, H.; Zhao, Y.; Hu, P. Analysis of influence of metro shield tunneling crossing underneath high speed railway. *Rock Soil Mech.* **2009**, *30*, 269–276.
10. Xu, Q.; Zhu, H.; Ma, X.; Ma, Z. Pile underpinning and removing technology of shield tunnels crossing through group pile foundations of road bridges. *Chin. J. Geo. Eng.* **2012**, *34*, 1217–1226.
11. Zhang, C.; Zhao, Y.; Zhang, Z.; Zhu, B. Case Study of Underground Shield Tunnels in Interchange Piles Foundation Underpinning Construction. *Appl. Sci.* **2021**, *11*, 1611. [CrossRef]
12. Li, P.; Zou, H.; Wang, F.; Xiong, H. An analytical mechanism of limit support pressure on cutting face for deep tunnels in the sand. *Comput. Geo.* **2020**, *119*, 103372. [CrossRef]
13. Mroueh, H.; Shahrour, I. Three-dimensional finite element analysis of the interaction between tunneling and pile foundations. *Int. J. Numer. Anal. Methods Geomech.* **2002**, *26*, 217–230. [CrossRef]
14. Lee, C.; Jacobsz, S. The influence of tunnelling on adjacent piled foundations. *Tunn. Undergr. Space Technol.* **2006**, *21*, 430. [CrossRef]
15. Liyanapathirana, D.; Nishanthan, R. Influence of deep excavation induced ground movements on adjacent piles. *Tunn. Undergr. Space Technol.* **2016**, *52*, 168–181. [CrossRef]
16. Wang, J.; Li, W.; Song, Z. Development and implementation of new triangular finite element based on MGE theory for bimaterial analysis. *Results Phys.* **2019**, *13*, 102231. [CrossRef]
17. Ayasrah, M.; Qiu, H.; Zhang, X. Influence of Cairo Metro Tunnel Excavation on Pile Deep Foundation of the Adjacent Underground Structures: Numerical Study. *Symmetry* **2021**, *13*, 426. [CrossRef]
18. Conte, E.; Pugliese, L.; Troncone, A.; Vena, M. A Simple Approach for Evaluating the Bearing Capacity of Piles Subjected to Inclined Loads. *Int. J. Geomech.* **2021**, *21*, 04021224. [CrossRef]
19. Achmus, M.; Thieken, K. On the behavior of piles in non-cohesive soil under combined horizontal and vertical loading. *Acta Geo.* **2010**, *5*, 199–210. [CrossRef]
20. Graine, N.; Hjiaj, M.; Krabbenhoft, K. 3D failure envelope of a rigid pile embedded in a cohesive soil using finite element limit analysis. *Int. J. Numer. Anal. Methods Geomech.* **2020**, *45*, 265–290. [CrossRef]
21. Jacobsz, S.; Standing, J.; Mair, R.; Hagiwara, T.; Sugiyama, T. Centrifuge Modelling of Tunnelling Near Driven Piles. *Soils Found.* **2004**, *44*, 49–56. [CrossRef]
22. Ng, C.; Lu, H.; Peng, S. Three-dimensional centrifuge modelling of the effects of twin tunnelling on an existing pile. *Tunn. Undergr. Space Technol.* **2013**, *35*, 189–199. [CrossRef]
23. Zheng, Y.; Xiong, J.; Liu, T.; Yue, X.; Qiu, J. Performance of a deep excavation in Lanzhou strong permeable sandy gravel strata. *Arab. J. Geosci.* **2020**, *13*, 156. [CrossRef]
24. Niu, D.; Zhang, L.; Fu, Q.; Wen, B.; Luo, D. Critical conditions and life prediction of reinforcement corrosion in coral aggregate concrete. *Constr. Build. Mater.* **2019**, *238*, 117685. [CrossRef]
25. Boonyarak, T.; Phisitkul, K.; Ng, C.W.; Teparaksa, W.; Aye, Z.Z. Observed ground and pile group responses due to tunneling in Bangkok stiff clay. *Can. Geo. J.* **2014**, *51*, 479–495. [CrossRef]
26. Liu, X.; Fang, Q.; Zhang, D.; Liu, Y. Energy-based prediction of volume loss ratio and plastic zone dimension of shallow tunnelling. *Comput. Geo.* **2019**, *118*, 103343. [CrossRef]
27. Wei, Y.; Guo, W.; Zhang, Q. A model for predicting evaporation from fresh concrete surface during the plastic stage. *Dry. Technol.* **2019**, *38*, 2231–2241. [CrossRef]

28. Li, P.; Chen, K.; Wang, F.; Li, Z. An upper-bound analytical model of blow-out for a shallow tunnel in sand considering the partial failure within the face. *Tunn. Undergr. Space Technol.* **2019**, *91*, 102989. [CrossRef]
29. Liu, X.; Fang, Q.; Zhang, D.; Wang, Z. Behaviour of existing tunnel due to new tunnel construction below. *Comput. Geo.* **2019**, *110*, 71–81. [CrossRef]
30. Cheng, W.-C.; Song, Z.-P.; Tian, W.; Wang, Z.-F. Shield tunnel uplift and deformation characterisation: A case study from Zhengzhou metro. *Tunn. Undergr. Space Technol.* **2018**, *79*, 83–95. [CrossRef]
31. Bilotta, E.; Russo, G. Use of a Line of Piles to Prevent Damages Induced by Tunnel Excavation. *J. Geo. Geoenvironmental Eng.* **2011**, *137*, 254–262. [CrossRef]
32. Harris, D.I.; Mair, R.J.; Love, J.P.; Taylor, R.N.; Henderson, T.O. Observations of ground and structure movements for compensation grouting during tunnel construction at Waterloo station. *Géotechnique* **1994**, *44*, 691–713. [CrossRef]
33. Xiang, Y.; Jiang, Z.; He, H. Assessment and control of metro-construction induced settlement of a pile-supported urban overpass. *Tunn. Undergr. Space Technol.* **2008**, *23*, 300–307. [CrossRef]
34. Bai, Y.; Yang, Z.; Jiang, Z. Key protection techniques adopted and analysis of influence on adjacent buildings due to the Bund Tunnel construction. *Tunn. Undergr. Space Technol.* **2014**, *41*, 24–34. [CrossRef]
35. Wang, Z.; Zhang, K.-W.; Wei, G.; Li, B.; Li, Q.; Yao, W.-J. Field measurement analysis of the influence of double shield tunnel construction on reinforced bridge. *Tunn. Undergr. Space Technol.* **2018**, *81*, 252–264. [CrossRef]
36. Wang, Z.; Xie, Y.; Liu, H.; Feng, Z. Analysis on deformation and structural safety of a novel concrete-filled steel tube support system in loess tunnel. *Eur. J. Environ. Civ. Eng.* **2019**, *25*, 39–59. [CrossRef]
37. Zhang, Y.; Zhang, D.; Fang, Q.; Xiong, L.; Yu, L.; Zhou, M. Analytical solutions of non-Darcy seepage of grouted subsea tunnels. *Tunn. Undergr. Space Technol.* **2019**, *96*, 103182. [CrossRef]
38. Kirsch, A.; Piazzi, L. Numerical investigation of the effectiveness of a bored pile wall for the minimisation of settlement resulting from tunnel driving. *Geomech. Tunn.* **2009**, *2*, 753–765. [CrossRef]
39. Lu, P.; Zheng, G.; Zhang, W.; Lei, H. Study on Risk Assessment and Fined Control of Influence of Shield Tunneling on Ground Surface Settlement: A Case Study on Tianjin Metro. *Tun. Con.* **2016**, *36*, 170–178.
40. Fang, M.; Liu, Z.; Zhou, C.Y.; Shi, H.O. Numerical simulation of influence of undercrossing shield construction on existing tunnel. *Railw. Eng. Sci.* **2011**, *8*, 67–72.
41. Surarak, C.; Likitlersuang, S.; Wanatowski, D.; Balasubramaniam, A.; Oh, E.; Guan, H. Stiffness and strength parameters for hardening soil model of soft and stiff Bangkok clays. *Soils Found.* **2012**, *52*, 682–697. [CrossRef]
42. Duncan, J.M.; Buchignani, A. *An Engineering Manual for Settlement Studies*; University of California: Oakland, CA, USA, 1976.
43. Mayne, P.W.; Kulhawy, F.H. K0-OCR relationships in soil. *J. Geo. Eng.* **1982**, *108*, 851–872.